



Realization of depth of field not limited by computational ghost imaging

Zhaohua Yang*, Yuzhe Sun, Ruitao Yan, Guanghan Li, Shaofan Qu

School of Instrumentation Science and Optoelectronic Engineering, Beihang University, Beijing 100191, China



ARTICLE INFO

Keywords:

Ghost imaging
Computational ghost imaging
Depth of field

ABSTRACT

Computational ghost imaging (CGI) presents a new way to solve the problem of extended depth of field (DOF), which has been studied for a long time. The application of correlation theory confirms that a plane light source can be used to avoid the limitation of DOF in CGI. Results from experiments where real objects are imaged by CGI between 0.3 m and 1.2 m verify that images are consistent in quality. This confirms that CGI is not affected by DOF and can be used to improve the accuracy of integral and microscopic imaging.

1. Introduction

Depth of field (DOF) refers to the range of distance, in which the camera lens or other imagers can obtain a clear image of the target. According to the theory of optical fluctuations, DOF is produced due to the diffusion circle after the lens, and its range is related to the focal length, numerical aperture, and object distance. In some cases, such as integral imaging [1] and microscopic imaging, DOF is a major problem limiting the image quality and accuracy. Various methods have been proposed to extend DOF, including wave-front coding [2] and light field camera [3]. However, these methods do not improve the limitation of DOF in principle.

Lensless imaging has been realized in ghost imaging (GI) [4], where the DOF is caused by the lens. Thus, this lensless system improves the DOF in principle. However, GI through a lens is more widely used, and little work has been performed on its DOF. Therefore, we report our research regarding the DOF of computational GI in this paper.

GI experiments attract considerable interest among researchers. It was once conducted by Y. H. Shi in 1994, where a GI setup was used for imaging a target by measuring the second-order correlation between the object arm and the reference arm [5]. The development of GI has three milestones: quantum GI (1994) [5–7], thermal GI (2002) [8], and computational GI (2009) [9]. Recent reports include a range of GI spanning the spectrum of electromagnetic and atomic waves, e.g., temporal GI [10], 3D GI [11], X-ray GI [12], and GI with atoms [13], all of which indicate a rapid development potential of GI. Characteristics of GI, such as super-resolution [14] and anti-interference [15,16], make it useful in application of lidars [17], precision imaging [18], optical encryption [19–21] and so on.

In ghost imaging, the influence of optical system on imaging is mainly divided into two aspects: object distance and focal length. In

traditional two-arm ghost imaging, the object distance has a great influence on the imaging, which needs to satisfy the condition that the distance from the light source to the object is equal to the distance from the light source to the detector. CGI breaks this limitation [9,22], which is a kind of single arm correlation imaging mode that uses structured light to illuminate target and collects the total light intensity at the object plane to perform correlation operations. In this paper, we investigate the DOF of CGI through theory and experiment and confirm that CGI with a plane light source can avoid the limitation of DOF.

2. Model and theory analysis

A system of CGI is shown in Fig. 1. The laser beam ($\lambda = 532$ nm) is expanded and clipped by a lens to meet a diameter of 3.5 cm. The expanded light passes through spatial light modulator (SLM), which modulates the light field by a series of matrices. The structured light field $E_0(\vec{r}, t)$ emitted from SLM is the light source and illuminates a mask with “BH”. The total reflected light $E_1(\vec{r}_1, t)$ from the mask is received by a bucket detector. In order to compare the DOF of charged coupled devices (CCDs) with CGI, a CCD is used as the bucket detector. The image of the object can be obtained from the second-order correlation function $G^2(\vec{r}, \vec{r}_1)$ between the source light field and the total reflected light. The distance from the target to the bucket detector is Z , and Z is varied at a gradient interval of 10 cm after imaging the object.

The second-order correlation $G^2(\vec{r}, \vec{r}_1)$ function between the light field and the total reflected light from target is

$$\begin{aligned} G^{(2)}(\vec{r}, \vec{r}_1) &= \langle E_0(\vec{r}) E_1(\vec{r}_1) E_1^*(\vec{r}_1) E_0^*(\vec{r}) \rangle \\ &= \langle I_0(\vec{r}) \rangle \langle I_1(\vec{r}_1) \rangle + |G^1(\vec{r}, \vec{r}_1)|^2, \end{aligned} \quad (1)$$

* Corresponding author.

E-mail address: yangzh@buaa.edu.cn (Z. Yang).

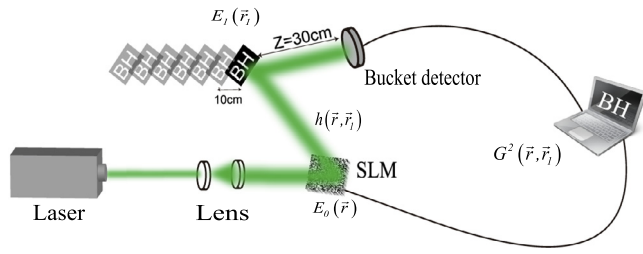


Fig. 1. Setup for the DOF of CGI.

where

$$\langle I_0(\vec{r}) \rangle = \int \langle E_0(\vec{r}, t) E_0^*(\vec{r}, t) \rangle d\vec{r}, \quad (2)$$

$$\langle I_1(\vec{r}_1) \rangle = \int h(\vec{r}, \vec{r}_1) h^*(\vec{r}, \vec{r}_1) \langle E_0^*(\vec{r}, t) E_0(\vec{r}, t) \rangle d\vec{r}, \quad (3)$$

and

$$G^1(\vec{r}, \vec{r}_1) = \int h^*(\vec{r}, \vec{r}_1) E_0^*(\vec{r}, t) E_0(\vec{r}, t) d\vec{r}. \quad (4)$$

$\langle I_0(\vec{r}) \rangle$ is the intensity of the light source, $\langle I_1(\vec{r}_1) \rangle$ the intensity of the object plane, and $G^1(\vec{r}, \vec{r}_1)$ the correlation function between the two light fields. The source field $E_0(\vec{r}, t)$ can be expressed as [23],

$$E_0(\vec{r}, t) = \sum_{m,n} \exp \left[-(\vec{r} - \vec{r}_{mn})^2 / (\vec{r} - \vec{r}_{mn})^2 r_c^4 \right] \exp [i\phi_{mn}(t)], \quad (5)$$

where \vec{r}_{mn} is the pixel position with a 2D index (m, n) and $\phi_{mn}(t)$ the modulated phase at time t with a range of $(-\pi, \pi]$. In Eq. (5), the intensity of each light beam is described as a Gaussian beam of radius r_c^2 . $h(\vec{r}, \vec{r}_1)$ is the transfer function, according to the propagation equation of the plane light field and can be expressed as

$$h(\vec{r}, \vec{r}_1) = \exp(ikz) t(x), \quad (6)$$

where k denotes wave number and $t(x)$ denotes the reflection function of the target. The light field $E_1(\vec{r}_1, t)$ of the object plane can be obtained by combining Eqs. (5) and (6), which is defined as $E_1(\vec{r}_1) = E_0(\vec{r}_0) \cdot h(\vec{r}, \vec{r}_1)$,

$$E_1(\vec{r}_1) = \sum_{m,n} \exp \left[-(\vec{r} - \vec{r}_{mn})^2 / (\vec{r} - \vec{r}_{mn})^2 r_c^4 \right] \cdot \exp [i\phi_{mn}(t) + ikz] \cdot t(x), \quad (7)$$

$I_0(\vec{r})$, $I_1(\vec{r}_1)$ and $G^1(\vec{r}, \vec{r}_1)$ can be obtained by substituting Eqs. (5) and (6) into Eqs. (2)–(4),

$$\langle I_0(\vec{r}) \rangle = \int \left| \sum_{m,n} \exp \left[-(\vec{r} - \vec{r}_{mn})^2 / (\vec{r} - \vec{r}_{mn})^2 r_c^4 \right] \right|^2 d\vec{r} = I, \quad (8)$$

$$I_1(\vec{r}_1) = I t^2(x), \quad (9)$$

$$|G^1(\vec{r}, \vec{r}_1)|^2 = I^2 t^2(x). \quad (10)$$

Substituting Eqs. (8), (9), and (10) into Eq. (1), we have

$$G^{(2)}(\vec{r}, \vec{r}_1) = 2I^2 t^2(x). \quad (11)$$

Information on the amplitude of the object can be obtained by measuring the second-order correlation of the two light fields. It can be seen from Eq. (11) that the image quality of CGI is not related to the distance Z . It can be concluded that CGI does not have a limitation of DOF. Note that there are two conditions to be met, one is the source should be a plane light source, and the other is that struttred light maintains parallel transmission. Comparing the source field $E_0(\vec{r})$ with the field at the object $E_1(\vec{r}_1)$, only the phase of the light field changes and the reflection function $t(x)$ of the target is comprised. The second-order correlation of

the light field is used to image the target; therefore, the phase change does not affect the imaging result. We theoretically demonstrated that CGI is not limited by the DOF.

3. Experimental results

Fig. 1 shows the object is the 12 mm × 20 mm mask containing the letter “BH”. The wavelength of the laser is 532 nm and it is modulated by an SLM with a frequency of 10 Hz, which is governed by 256 × 256 Hadamard matrices. Due to the huge amount of data, we divided the 256 × 256 image into sixteen 64 × 64 image. FPGA with parallel characteristic is used to control timing and synchronous calculation, making generation of matrix is synchronized with the reconstructed calculation and implement fast parallel computation, which can increase the speed of calculation. The object is imaged at 10 different distances separately to investigate if there is any limitation of the DOF in CGI. The initial distance from the detector to the target is 0.3 m, and a reconstructed image of 256 × 256 pixels are obtained from 65,536 exposures. We change the distance Z from 0.3 m to 1.2 m with an interval of 10 cm and 10 images are shown in Table 1.

It is clear from Table 1 that images obtained by CGI have no DOF blur at different distances. With increasing distance, images of CCD gradually blurred and the object is out of recognition at 1.2 m. However, the image quality of CGI remains consistent from 0.3 m to 1.2 m. The absence of diffused circles indicates that CGI has no limitation in DOF.

After comparing the results of CGI and CCD obtained at different distance, we compare the image quality at different distances by plotting the cross section of letter “H”, the section looks like a double slit and contains 130 pixels, which are marked with red in Fig. 2(a), the double slit is 1.5 mm wide and its spacing is 4.5 mm. The double slit width of four images: 0.3 m, 0.6 m, 0.9 m, and 1.2 m are shown in Fig. 2(b).

Fig. 2(b) shows that width of the letter “H” remains unchanged when the distance changes, moreover, the edges of the letter “H” in the four images all change vertically. If there is DOF blur in CGI, the results will be different, i.e., the letter will appear widened and the edge gradually decreased with the distance changing. The double slit intercepted from letter “H” indicates no limitation of DOF.

Signal-to-noise ratio (SNR) and contrast-to-noise ratio (CNR) can be used to evaluate the quality of the image from another aspect. They are defined as [24]

$$SNR = \frac{\sum_{(m=1,n=1)}^{(m=256,n=256)} \left(U_0(m, n) - \frac{1}{m \times n} \sum_{(m=1,n=1)}^{(m=256,n=256)} U_0(m, n) \right)^2}{\sum_{(m=1,n=1)}^{(m=256,n=256)} (U(m, n) - U_0(m, n))^2}, \quad (12)$$

where (m, n) denotes the pixel coordinates in the image, $U_0(m, n)$ the original image, and $U(m, n)$ the CGI image, which are shown in Fig. 3(b).

$$CNR = \frac{\langle G(x_s) \rangle - \langle G(x_b) \rangle}{\sqrt{\Delta^2 G(x_s) - \Delta^2 G(x_b)}}, \quad (13)$$

where $G(x_s)$ and $G(x_b)$ denote the target intensity and background intensity separately, and $\Delta^2 G(x) = \langle G^2(x) \rangle - \langle G(x) \rangle^2$ represent the variance of intensity. The SNR and CNR of 10 images are shown in Fig. 3(a). The SNR shows a fluctuation caused by the equipment noise, fluctuation of the light source, and the original image error caused by manufacturing and is independent of distance. The CNR shows the degree of contrast between the target and the background and it is not affected by Z , either. Fig. 3(a) shows there is little difference in SNR and CNR quantitatively and the image quality is not affected by DOF.

Experimental results show that the CGI system used by us does not limit DOF from different aspects. First, we compared the CCD and CGI image results at a distance between 0.3 m and 1.2 m. We then conducted internal comparison in CGI through double slit widths. Finally, we use

Download English Version:

<https://daneshyari.com/en/article/7924849>

Download Persian Version:

<https://daneshyari.com/article/7924849>

[Daneshyari.com](https://daneshyari.com)